

# Energy Detection Based Spectrum Sensing for Rural Area Networks

Johanna Vartiainen<sup>1,\*</sup>, Heikki Karvonen<sup>1</sup>, Marja Matinmikko-Blue<sup>1</sup>, Luciano Mendes<sup>2</sup>, Harri Saarnisaari<sup>1</sup>, Alexandre Matos<sup>3</sup>

<sup>1</sup>Centre for Wireless Communications, University of Oulu, Finland

<sup>2</sup>Radiocommunications Research Center, Inatel, Brazil

<sup>3</sup>Federal University of Ceará, Brazil

## Abstract

Remote and rural areas are a challenge to deploy cost-efficient connectivity solutions. 5G technology needs lower frequencies, which calls for spectrum sharing for local networks. Spectrum sensing could complement traditional database approach for spectrum sharing in these areas. This paper studies a windowing based (WIBA) blind spectrum sensing method and compares its performance to a localization algorithm based on double-thresholding (LAD). Both methods are based on energy detection and can be used in any band for detecting rather narrowband signals. Probabilities of detection and false alarm, relative mean square error, number of detected signals and detection distances were evaluated in multipath, multi-signal and rural area channel conditions. The simulation results show that the WIBA method is suitable for 5G remote areas, due to its good detection performance in low signal-to-noise ratios (SNR) with low complexity. Results also show importance of the detection window selection.

Received on 30 October 2019; accepted on 12 March 2020; published on 07 April 2020

**Keywords:** signal detection, spectrum utilization, 5G system, overlapping, energy detector.

Copyright © 2020 J. Vartiainen *et al.*, licensed to EAI. This is an open access article distributed under the terms of the Creative Commons Attribution license (<http://creativecommons.org/licenses/by/3.0/>), which permits unlimited use, distribution and reproduction in any medium so long as the original work is properly cited.

doi:10.4108/eai.7-4-2020.163923

## 1. Introduction

5th generation (5G) mobile communication networks present an evolution in the cellular network development bringing enhanced mobile broadband connectivity like discussed in CROWNCOM 2019 [1]. 5G networks target higher spectrum efficiency, lower latency, improved scalability and new application areas in digitalizing different sectors. One important application area is to connect a large number of objects, such as sensors and machines, to the Internet of Things (IoT) [2]. Spectrum is the critical resource for the deployment of 5G networks. In the first stage, 5G networks are planned to be deployed in higher carrier frequencies compared to existing cellular networks including 3.5 GHz and 26/28 GHz bands. Traditionally, cellular networks have been deployed in exclusively licensed bands where existing spectrum users have been moved to other bands, thus clearing the bands for cellular

networks. In 5G, different spectrum access models are considered in different countries including nation-wide licenses, local licenses and license-exempt operations. In some cases, the incumbent primary users (PU) are protected from harmful interference from the cellular networks when clearing the band has turned out to be difficult.

5G deployments are primarily targeting urban areas especially since operations in the higher carrier frequencies restrict the propagation distances significantly. Remote and rural areas present a challenge for deployment and the low population densities restrict investments. 5G-RANGE project [3] has proposed alternative deployment models especially for remote and rural areas where different stakeholders could deploy a regional network through shared spectrum access. The primary user must not be interfered by the entrant secondary users (SU). Spectrum sharing could be possible in areas where the incumbent users are not using the band which could particularly be the case in remote and rural areas. Typically, databases and spectrum

\*Corresponding author. Email: [johanna.vartiainen@oulu.fi](mailto:johanna.vartiainen@oulu.fi)

sensing techniques are proposed to be used to protect the existing spectrum users from harmful interference, see e.g. [4–7]. Databases are typically used to collect and store information about licensed users, such as TV and program making and special events (PMSE) signals (e.g. wireless microphone signals) for TV White Space (TVWS) access in some geographical areas [8, 9]. Spectrum sensing can be used to find out (detect) which frequency bands are being used by observing the radio environment. Approaches to combine databases with spectrum sensing exist where the sensing results are used to detect specific primary users [10], or make sensing results available through a database [11].

In 5G scenarios, database-driven spectrum sharing approaches have been proposed [5, 12]. Spectrum sensing could be used to enhance the traditional database approach by bringing more accurate information about the actual spectrum usage and thus increase the potential and reliability of shared spectrum access. 5G network related application areas for spectrum sensing include, e.g., mobile cellular systems [13], device-to-device (D2D) communication [14], and IoT [15]. Spectrum sensing can be used when the information in database or from geolocation method (like GPS) is inaccurate, or there is no connection to the database at all, like in disaster-related events or in remote areas. One important application area for spectrum sensing is when multiple SUs share the spectrum. In that case they could use sensing to determine if other SUs are present [16]. 5G can be tailored to be used for remote area connectivity where the use of TVWS, i.e., Very High Frequency (VHF) and Ultra High Frequency (UHF) bands, with database can be enhanced with spectrum sensing. In rural and remote areas the challenge is that distances are long and, thus, signal-to-noise ratio (SNR) levels are low, which makes their detection difficult.

5G networks aim at connecting a large number of devices, especially in IoT scenarios, while keeping design complexity and costs in a reasonable level. Energy detection (ED) is a cost-efficient sensing technique that is recommended to be used especially in cooperative sensing, where users collaborate and exchange their sensing information [17]. 5G cooperative sensing based on ED methods has been studied, for example, in [18]. The problem is that conventional ED does not perform well at low SNR values.

In this paper, the performance of an efficient and blind ED-based spectrum sensing method, namely the windowing based (WIBA) signal detection method [19], is studied. The WIBA method uses overlapping blocks in spectrum sampling to increase its detection performance. The widely studied localization algorithm based on double-thresholding (LAD) method [20], which has been found to outperform conventional ED methods [21], is used as a point of comparison. In [19], probability of detection vs. SNR as well as the number

of detected signals in one-signal case were studied in an Additive White Gaussian Noise (AWGN) channel. In [1], AWGN and multipath sensing were considered, and the effect of the detection window length  $M$  to the detection performance in different channel situations was studied. In addition, relative mean squared error (RMSE) for the bandwidth estimation, as well as detection probability over multipath channels, were considered. Single and cooperative sensing detection distances in a rural channel were studied in [22] and [23], respectively. Detection distance is the maximum distance between the transmitter and the receiver on which the signal can be detected. Here, paper [1] is extended to cover also false rate alarm analysis of the WIBA and the LAD methods. In addition, detection distance results in Free Space Path Loss (FSPL) AWGN channel are presented and compared with those achieved using rural channel model.

This paper is organised as follows. In Section 2, system model including 5G rural area channel model is presented. Section 3 considers spectrum sensing, the WIBA and the LAD methods, as well as false alarm rate analysis. Numerical results are presented in Section 4 and conclusions are drawn in Section 5.

## 2. Rural area scenario

### 2.1. Motivation

Connectivity in rural and remote areas is a true challenge because most of today's technologies are restricted to coverage areas whose radius is below 10 km. In a sparsely populated area, a cell with 10 km radius will only cover a small number of subscribers, resulting in very high fees per user. Another problem for realizing remote connectivity today is the high cost of the spectrum licenses, which restricts who can obtain a license to deploy a cellular network. At the same time, it increases the investments to deploy a mobile network and hinders its economic feasibility. 5G in remote areas requires the use of lower frequency bands to reach wider area coverage, e.g., 50-100 km. Figure 1 illustrates example use case scenarios for remote area networks. Remote area network could be used to provide wireless broadband connection, e.g., to a remote village residents, rural smart farms and mining locations, by using a large cell with 50 km cell radius. In addition, long-range links could be used as a wireless backhaul to provide connection to remote locations which does not have a fiber available. Due to long-range links, the upcoming 5G millimeter wave bands are not the first options for connectivity in remote areas. Instead, the use of TVWS or other bands below 1 GHz have the potential to be used by 5G networks for providing cost-efficient solution in remote areas. While TVWS research peaked about a decade ago, their deployments are still limited.

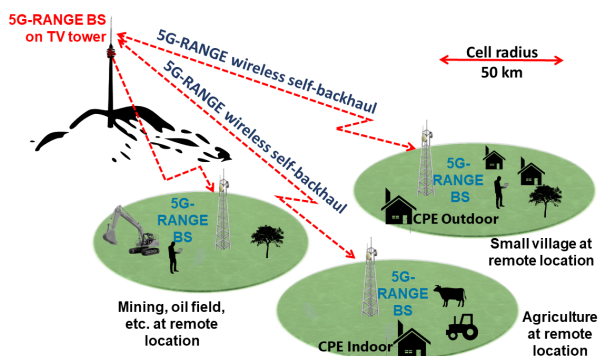


Figure 1. Example remote area scenarios.

Administrations have developed rules for the use of TVWSs and typically selected a geolocation database approach as the means to protect the incumbent TV broadcasting usage, see e.g. [24]. In these approaches, devices wishing to access the TVWS need to inquire a database and report their location to be allowed to use a channel. The database is in charge of ensuring that the incumbents are protected. While there is some research on the use of spectrum sensing to complement database approach in TVWS, it has not been adopted so far.

One example of the shared spectrum access is the Citizen Broadband Radio Service (CBRS) by the Federal Communications Commission (FCC) for the 3.5 GHz band. CBRS introduces locally licensed or license-exempt operations while protecting the incumbent spectrum users, such as the incumbent military radars and fixed satellite stations [10]. The CBRS system is based on a database approach and it additionally includes the use of spectrum sensing to avoid interference to/from military radar systems.

The opportunistic use of the TVWS or any other spectrum sharing arrangement typically requires that the incumbent spectrum users are protected. While there are standards that employ cognitive radio approaches based on geolocation database to inform the base station (BS) about the spectrum opportunities in a given region, spectrum sensing techniques can be used in conjunction with the database approach to enhance the reliability and increase shared spectrum access opportunities. In fact, the presence of unofficial TV transmitters is a reality in some countries where remote area connectivity is a challenge. Pirate TV stations are unlikely to be included in the geolocation database and it can hinder the operation of the secondary network assigned to operate by the geolocation database in a frequency band occupied by an unauthorized TV broadcaster. Database information may be inaccurate due to software based propagation estimation, which can lead to erroneous results in varying terrain shapes that are present in remote area scenarios. Spectrum

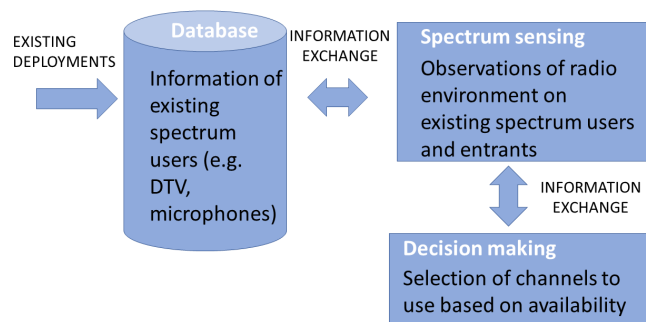


Figure 2. System model for spectrum sensing to complement database approach.

sensing will be used also to detect other SUs at the same region. In addition, there are situations where the use of spectrum sensing can provide benefits such as in the presence of unauthorized transmissions (e.g., pirate TV transmissions). Figure 2 summarizes the high-level system model for the combined spectrum sensing and database approach. In the 5G-RANGE project [3], this approach is proposed specifically for rural and remote areas to dynamically exploit free spectrum holes available at TV bands.

## 2.2. System model

In our system model, it is considered a remote area comprising a single cell with 50 km of radius. Due to large cell size, it can include various different terrains and vegetation. On the other hand, rural areas do not have tall buildings that would block or reflect the signal transmissions. In any case, rural and remote area communication system development and performance estimation requires a dedicated channel model. In this work, a rural area channel model, which is developed based on the real measurements [25], is used when evaluating the performance of spectrum sensing. Delay spread and path loss measurements were done in rural areas of Australia in four different scenarios with link distance until 200 km to include the effect of varying terrains. Based on the measurement results, a rural channel model has been developed including path loss and multi-path fading characteristics. The path loss model for 50 km cell radius was defined to be [26]

$$PL(d, f) = P_{FS}(d, f) + K, \quad (1)$$

where  $d$  is the distance,  $f$  is the central frequency,  $P_{FS}(\cdot)$  is the free space path loss model, and  $K = 29.38$  is an offset which minimizes the mean squared error (MSE)  $\bar{\epsilon}(K)$  between the proposed path loss in (1) and the measured path loss samples in [25]. The minimum value for  $\bar{\epsilon}(K)$ , i.e.,  $\bar{\epsilon}(29.38)$  provides the standard deviation  $\sigma_{SF}$  which is equal to 4.47 dB [27].

To include the small scale fading parameters to the channel model, the recommendations from [28], the measured delay spread in [25], and the 3rd Generation Partnership Project (3GPP) Clustered Delay Line (CDL)-A model [29] were used [27]. Finally, a detailed description of the channel model used in this paper can be found in [27].

### 3. Spectrum Sensing

Mobile user equipment (UE) are expected to perform sensing to find out free spectrum opportunities. Therefore, in this work, ED-based spectrum sensing method is selected to enable feasible implementation complexity in the UEs. This section describes the studied WIBA energy detection method, which is considered to be used for rural area spectrum sensing. In the performance evaluation, a well-known LAD method [20, 21] is used as a reference for comparison and it will also be introduced shortly in this section.

Both the methods are blind spectrum sensing algorithms that are able to estimate the noise level iteratively by using adaptive thresholds. They can be applied to a wide set of situations since ED method does not require *a priori* knowledge of the characteristics of the signal to be detected. However, a downside of the simplicity is that the signals to be detected must be narrowband with respect to the analyzed bandwidth (BW). The narrower the signal, the better the methods will perform, hence it is reasonable to make an assumption that the signal's BW has to be at most 50% of the analyzed BW [19, 21]. According to [21], as the signal's BW gets wider, SNR must be higher in order to achieve an acceptable sensing performance. Note, that the methods are not frequency dependent, i.e., they can be used in any frequency band (kHz-GHz).

The signal detection is based on the estimated noise level, therefore information about the noise level or present signal(s) are not needed. The noise is assumed to be a white Gaussian process. Even though the assumption is that the noise is Gaussian, it has been shown that the signal can be found even if the noise is not purely Gaussian [21]. A detection threshold is used to divide received samples into two sets: one set contains estimated noise-only samples, and another set contains estimated signal samples and noise. Threshold selection is addressed by the constant false alarm rate (CFAR) principle, which means that the used detection threshold parameter is calculated *a priori* using a predefined desired false alarm rate  $P_{fa}$  and the statistical properties of the noise [30, 31].

In this paper, it is assumed that the samples  $x_i$ , taken in the frequency-domain are zero mean, independent and identically distributed (i.i.d.) Gaussian complex random variables. The energy of sample  $x_i$  is  $y_i = |x_i|^2$ , which follows a chi-squared distribution. By assuming

**Table 1.** Threshold parameter values  $T$  for different  $P_{fa}$  and  $M$  values.

$P_{fa}$	$M = 1$	$M = 4$	$M = 10$	$M = 100$
0.1	2.303	1.670	1.512	1.130
0.01	4.605	2.511	1.878	1.247
0.001	6.908	3.266	2.266	1.338

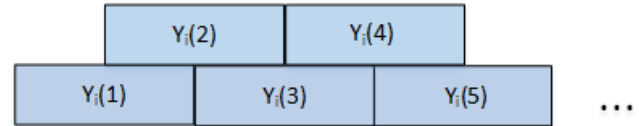


**Figure 3.** Illustration of 50% overlapping when there are  $L$  overlapping blocks and the length of one block is  $M$ .

chi-squared distributed variables with  $2M$  degrees of freedom, the threshold parameter  $T$  can be found by solving [32–34]

$$P_{fa} = e^{-TM} \sum_{k=0}^{M-1} \frac{1}{k!} (TM)^k, \quad (2)$$

where  $P_{fa}$  is the pre-selected false alarm rate. Note that (2) does not depend on the noise variance. When  $M = 1$ , variables follow chi-squared distribution with two degrees of freedom, and (2) leads to a threshold parameter

$$T = -\ln(P_{fa}), \quad (3)$$

which corresponds to LAD method case. Example threshold parameter values  $T$  for different values of  $P_{fa}$  and  $M$  are presented in Table 1. Note that the threshold parameter is constant for specific  $M$  and  $P_{fa}$ , and can be calculated beforehand.

#### 3.1. The WIBA Method

In the WIBA method, overlapping is used in spectrum sampling. Assume that  $N$  energy samples  $y$  are obtained during the channel sensing. The observed samples are divided into  $L$  overlapping blocks (i.e. detection windows) with length  $M$ . An example case, where the degree of overlapping between two blocks is 50%, is illustrated in Figure 3. Samples in each block are summed up among themselves, so each block  $Y_i(l)$ ,  $l = 1, \dots, M$  consists of samples  $\frac{kM}{2} + 1, \dots, \frac{kM}{2} + M$ ,  $k = 0, \dots, L - 1$ . The signal detection threshold is [19]

$$T_h = T \frac{1}{L} \sum_{i=1}^L Z_i, \quad (4)$$

where  $T$  comes from (2) and  $Z_i$  is the total energy in  $i$ th block, i.e.,  $Z_i = \sum_{l=1}^M Y_i(l)$  when  $i = 1, 2, \dots, L$ .

### 3.2. The LAD Method

The LAD method [20, 21] utilizes iterative forward consecutive mean excision (FCME) threshold setting process. In the FCME process, energy samples  $y$  are rearranged into an ascending order according to their sample energy. After that,  $n = 10\%$  of the smallest samples in energy are selected to form the initial set  $Q$ . The used threshold is calculated using  $T_h = T\bar{y}$ , where threshold parameter  $T = -\ln(P_{fa})$  comes from (3),  $P_{fa}$  is the pre-selected false alarm rate and  $\bar{y}$  is the mean of energy samples. In the first iteration, mean is calculated from the initial set  $Q$ . The samples below the threshold are added to the initial set, and this iterative process continues until there are no samples below the threshold. After the last iteration, samples below the threshold are from noise and samples above the threshold are detected signal samples. Threshold setting procedure is described in more details, e.g., in [33].

The LAD method uses two FCME thresholds, namely the upper ( $T_{h,up}$ ) and the lower ( $T_{h,low}$ ) ones. The lower threshold helps avoiding separating a signal as the upper threshold is used to avoiding false detections. After calculating the upper and lower a thresholds using two different threshold parameters,  $T_u$  and  $T_l$ , the LAD method uses clustering to group adjacent samples assumed to be from the same signal. The LAD method clusters together adjacent samples above the lower threshold  $T_{h,low}$ . The cluster is accepted to be caused by a signal if at least one of the samples is also above the upper threshold  $T_{h,up}$  (so called detection threshold). The performance of the LAD method can be improved using an adjacent cluster combining (ACC) parameter that allows  $p$  (usually  $p = 3$ ) samples to be below the lower threshold between two accepted clusters [21].

### 3.3. False Alarm Rate Analysis

Probability of false alarm (i.e. false alarm rate) is a probability of incorrectly detecting that the signal is present even though there is no signal present. In other words, channel is found to be occupied even though it is not, and then possibility to use a vacant channel is lost. The larger the false alarm probability is the higher is the number of lost spectrum opportunities.

The LAD and WIBA methods are CFAR methods which use predetermined, constant false alarm rate in the threshold setting process. This predetermined false alarm rate is called as a desired false alarm rate ( $P_{fa,des}$ ). As introduced above, the LAD uses two and the WIBA method uses only one threshold. In the case of the LAD method, commonly used typical desired false alarm probability for the detection (upper) threshold is  $P_{fa,desLAD} = 10^{-6}$  [21], and in the case of the WIBA method, it is  $P_{fa,desWIBA} = 0.01 = 10^{-2}$  [19]. The reason why the methods use different false alarm probabilities

is caused by the different operating principles of the methods. As the resulting threshold for the LAD ACC method is fixed, the resulting threshold for the WIBA method depends on the length of the block  $M$ . In addition, the LAD ACC method uses two desired false alarm probability values to get two detection thresholds as the WIBA method uses only one desired false alarm probability value and, thus, only one detection threshold. When using those values, the results are not fully comparable with each others. For accurate comparison of the LAD and WIBA methods, equal  $P_{fa,des}$  values are defined next to enable performance difference evaluation.

Let us assume that we have a one signal experiment with length of  $N$  samples. The experiment consists of  $K$  threshold comparisons (tests). Total false alarm rate  $P_{FA}$  is the desired false alarm rate multiplied by he number of tests, i.e.,

$$P_{FA} = P_{fa,des}K. \quad (5)$$

The LAD method compares every sample to the threshold. Thus, length of one test is one, and one experiment consists of  $K = N$  tests (Figure 4). If  $P_{fa,desLAD} = 10^{-6}$  is the desired false alarm rate in one test and  $N = 1024$ , it follows from (5) that the total false alarm rate for the LAD method is

$$P_{FA,LAD} = P_{fa,desLAD}N = 10^{-6}1024 \approx (10)^{-3}. \quad (6)$$

The WIBA method divides signal into  $L$  overlapping blocks with length  $M$  and sums up samples in each block so that each block produces one value that is compared to the threshold. Each test can be seen as the energy of  $M$  samples. Therefore, in one experiment there are  $K = L$  tests. Without overlapping,  $L = N/M$ . With 50% overlapping, there are approximately  $L = 2(N/M)$  tests, because 50% overlapping approximately doubles the number of blocks (Figure 4). If  $P_{fa,desWIBA} = 10^{-2}$  is desired false alarm rate in one test, it follows from (5) that the total false alarm rate for the WIBA method is

$$P_{FA,WIBA} = P_{fa,desWIBA}L = 10^{-2}L. \quad (7)$$

Because  $P_{FA,LAD} = P_{FA,WIBA}$ ,  $P_{FA,LAD} = P_{fa,desWIBA}L$ , and it follows that desired false alarm rate in one test for the WIBA method is

$$P_{fa,desWIBAnew} = P_{fa,desWIBA} = P_{FA,LAD}/L = 10^{-3}/L. \quad (8)$$

Therefore, in the simulations, (8) is used to have an accurate comparison. False alarm rate  $P_{fa,desWIBAnew}$  depends on the number of the overlapping blocks  $L$ . Corresponding values for some signals are presented in Table 2. For example, when  $M = 102$  and  $L = 20$ ,  $P_{fa,desWIBAnew} = 10^{-3}/20 = 5 \times 10^{-5}$ .

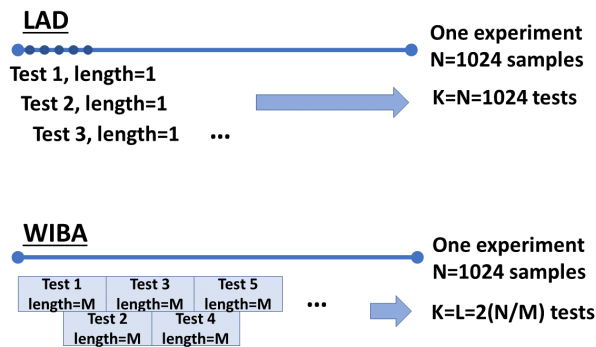


Figure 4. Tests in one experiment.

Table 2. Corresponding LAD false alarm rate values  $P_{fa,desWIBANew}$  for the WIBA method for different values of  $L$ .

$M$	$L$	$P_{fa,desWIBANew}$
52	39	$2.5 \times 10^{-5}$
102	20	$5 \times 10^{-5}$
204	10	$10^{-4}$

#### 4. Simulation Results

In the computer simulations, the WIBA method was studied and compared to the well-studied LAD method with ACC parameter (LAD ACC) which has been found to outperform general ED methods [20, 21, 33]. In detection performance simulations, it is desired that the detection probability  $P_d$  is as large as possible. Here, typical requirement that  $P_d \geq 0.9$  is used [3]. The probability of detection  $P_d$  is defined so that the signal is defined to be detected if threshold is crossed at its center frequency. The measured signal, occupying 5 – 30% of the channel BW, was based on binary phase-shift keying (BPSK) modulation. The BPSK signal was band-limited by a raised-cosine (RC) filter with a roll-off factor of 0.22. The BPSK signal is used as a general signal, because modulation methods etc. have no effect to the detection probability of the WIBA and LAD ACC methods [21]. In Figure 5, there are two measured WLAN signals at 2.45 GHz, as an example. As can be seen, both the methods find the signals. The number of frequency domain samples  $N = 1024$ . SNR was defined as a total signal power per total noise power, i.e., over  $N$  samples. The amount of Monte Carlo iterations was 1000. The WIBA method used  $P_{FA} = 0.01$ , 50% overlapping,  $M$  varied, and  $L \approx 2 \frac{N}{M}$ , unless otherwise stated. The used threshold parameter  $T$  depends on  $M$  as shown in Table 1. Detection window length  $M$  was defined to be optimal when it equals to the signal bandwidth. Table 3 shows optimal detection window

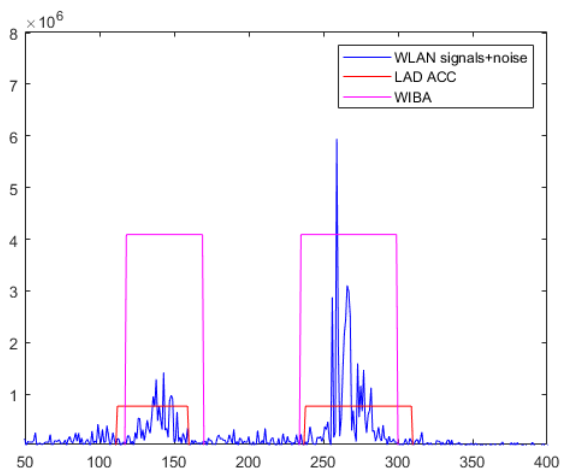


Figure 5. Measured WLAN signals detected using the LAD ACC and WIBA methods.

lengths  $M$  for signals with different bandwidths. For example, window length  $M = 52$  samples is optimal for signal with 5% BW (= 52 samples). The LAD threshold parameters were 13.81 (upper;  $P_{FA} = 10^{-6}$ ) and 2.66 (lower;  $P_{FA} = 0.07$ ) [21], and  $M = 1$  (=no windowing). An adjacent version of the LAD method with ACC parameter  $p = 3$  was used.

At first, detection performance vs. SNR was studied in an AWGN and multipath channels [1]. The effect of the detection window length  $M$  to the detection performance in different channel situations was studied. RMSE for the bandwidth estimation was evaluated, as well as detection probability over multipath channels in multi-signal situations. Results are presented in Sections 4.1-4.3. Secondly, detection performance vs. detection distance in kilometers [km] was studied in a FSPL AWGN and 5G rural area channels. Detection distance is the maximum distance between the transmitter and the receiver on which the signal can be detected, i.e.,  $P_d \geq 0.9$  is achieved. Results of the detection distance are presented in Section 4.4. Finally, the effect of false alarm rate is studied in Section 4.5.

##### 4.1. One Signal Scenario

In [19], an initial performance evaluation of WIBA was done by studying the probability of detection and the number of detected signals in one-signal case. Based on those results it was concluded that a very long window is preferred instead of the very short one when considering performance in terms of  $P_d$ .

In this paper, BW estimation accuracy is studied. Relative mean square error (or root mean squared relative error, RMSRE) of BW estimation is defined to

**Table 3.** Optimal detection window lengths  $M$  for signals with different bandwidths (samples / %).

Detection window length $M$	signal BW samples / %
10 samples	BW 10 samples / 1%
40 samples	BW 40 samples / 4%
52 samples	BW 52 samples / 5%
102 samples	BW 102 samples / 10%
204 samples	BW 204 samples / 20%
306 samples	BW 306 samples / 30%

**Table 4.** Relative Mean Square Error (RMSE) [%] in the one signal scenario for 10, 20, and 30% bandwidth when  $M = 52, 102, 204$  and  $306$ .

BW % (samples)	WIBA, $M =$				LAD ACC
	52	102	204	306	
BW 10% (102)	58	<b>100</b>	300	500	8
BW 20% (204)	15	50	<b>100</b>	198	6
BW 30% (306)	7	15	33	<b>100</b>	13

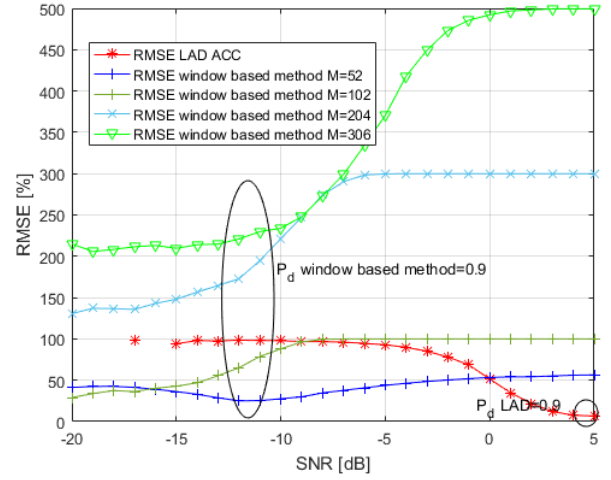
be

$$RMSE_{\gamma} = \sqrt{\frac{1}{N} \sum_{i=1}^N \left( \frac{\gamma_i - \hat{\gamma}_i}{\gamma_i} \right)^2}, \quad (9)$$

where  $\gamma_i$  is the BW and  $\hat{\gamma}_i$  is the estimated BW.

Table 4 shows the results when there is one signal with 10, 20 or 30% BW, and  $M = 52, 102, 204$  and  $306$ . Results for optimal window lengths are in bold. For example, when the signal BW is 10% and  $M = 102$ , RMSE is 100% for WIBA method. On the other hand, RMSE for LAD ACC method is only 8%. It can be noticed that using WIBA method, too long window degrades the BW estimation accuracy because in that case, the detected signal does not cover the whole window. For example, when BW= 10% and the detection window length  $M = 306$ , the detected signal covers only one third of the WIBA detection window. The LAD ACC method has better BW detection accuracy than the WIBA method because in the LAD ACC method, there is no detection window but the detection is performed one sample at a time.

In Figure 6, RMSE vs. SNR is presented for a signal occupying 10% of the overall BW (corresponding to the first line in Table 4). It can be seen that the WIBA method with optimal window length ( $M = 102$ ) operates well, and the larger the SNR, the better the LAD ACC method performs. Figure 6 also shows at which SNR values each method achieve  $P_d = 0.9$ . Note that the WIBA method has  $P_d = 0.9$  when


**Figure 6.** RMSE vs. SNR results for the case when bandwidth of the signal is 10%.

$-13 \text{ dB} \leq \text{SNR} \leq -11 \text{ dB}$ , depending on the  $M$ , while the LAD ACC method achieves  $P_d = 0.9$  when  $\text{SNR} = 5 \text{ dB}$ . That is, the performance difference is 16 – 18 dB. Because the WIBA method is able to operate in low SNR region ( $\text{SNR} < -10 \text{ dB}$ ), it is feasible for remote area scenarios, where long distance propagation makes received signal's strength weak. However, the LAD method has better BW estimation accuracy. It can be seen that, for the WIBA method, RMSE rises with the SNR when  $M$  is large. This is because the fact that as the detection performance of the LAD method depends on the bandwidth of the detected signal, the detection performance of the WIBA method depends also on the length of the used detection window. For example, when  $M = 204$  and  $M = 306$ , they are two (three) times wider than the optimal window ( $M = 102$ ), so the bandwidth has been estimated to be much wider than it is.

## 4.2. Multi-Signal Scenario

In this scenario, it is assumed that two RC-BPSK signals are present in the channel. The results are presented in Table 5, considering that there are one or two signals occupying 10% and 5% of the channel's BW, respectively. For example, when  $M = 102$  and there are two signals with BWs corresponding to 10% and 5%, the performance of the WIBA method is at most 1 dB worse when compared to the one signal scenario. Optimal values for  $M$  are 102 for 10% BW signal and 52 for 5% BW signal. Note that  $M$  does not affect the LAD ACC performance because there is no windowing. Based on Table 5, multi-signal situation has only slight effect to the performance of the methods.

In Figure 7, the number of detected signals vs. SNR is presented. There are two signals with 5% and 10%

**Table 5.** Required SNR [dB] for  $P_d = 0.9$  when there is one or two signals present.

Window length $M$	# of signals	Signal BW	WIBA method $P_d = 0.9$	LAD ACC method $P_d = 0.9$
$M = 102$	Two	10%	-13 dB	3 dB
		5%	-13 dB	-1 dB
$M = 102$	One	10%	-13 dB	1 dB
		5%	-14 dB	-2 dB
$M = 52$	Two	10%	-12 dB	3 dB
		5%	-14 dB	-1 dB
$M = 40$	Two	10%	-11 dB	3 dB
		5%	-14 dB	-1 dB
$M = 10$	Two	10%	-5 dB	3 dB
		5%	-10 dB	-1 dB
$M = 10$	One	10%	-5 dB	1 dB
		5%	-11 dB	-2 dB

BWs, and  $M = 10, 40, 52, 102$  and  $204$ . The results are the average of a thousand tests (Monte Carlo trials). The LAD ACC method starts to operate properly when  $\text{SNR} > -5$  dB. The LAD ACC method and the WIBA method with too short window ( $M = 10$ ) overestimate the number of signals when SNR is close to their sensitivity limit. Therein, the rising sidelobes can cause falsely detected signals. However, with SNR higher than that, the methods start to operate properly again. In the case of the WIBA method, the optimal window size gives correct estimates for the number of signals most of the time. This figure also shows at which SNR each approach achieves  $P_d = 0.9$ . For example, when  $M = 52$ ,  $P_d = 0.9$  when  $\text{SNR} = -12$  dB. The window is very short when  $M = 10$  and  $M = 40$ . Optimal window lengths are  $M = 52$  for 5% BW signal and  $M = 102$  for 10% BW signal. When  $M = 40, 52$  and  $102$ , the WIBA method estimated the number of signals correctly when  $P_d = 0.9$ . It can be seen that too short window ( $M = 10$ ) estimates the number of detected signals correctly only when SNR is larger: when  $P_d = 0.9$  ( $\text{SNR} = -5$  dB), the number of detected signals is 2.7 on average, and achieves 2 when  $\text{SNR} = 1$  dB. This corresponds the behaviour of the LAD ACC method. When using the LAD ACC method, the number of detected signals is about 2.2 on average at its best, assuming the SNR range analyzed in Figure 7. As can be seen from Figure 8, the BW estimation accuracy of the WIBA method may suffer if the window is too wide ( $M = 204$ , for instance). Too large  $M$  leads to that closely spaced signals can be seen as one signal by the sensing technique.

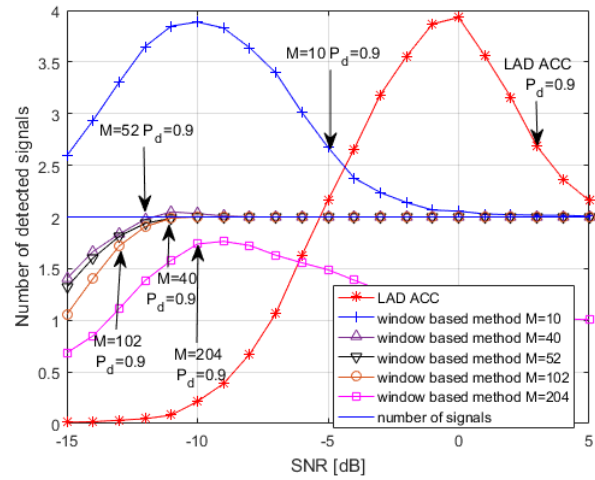


**Figure 7.** Number of detected signals vs. SNR results. There are two signals with 10% and 5% bandwidths to be detected.

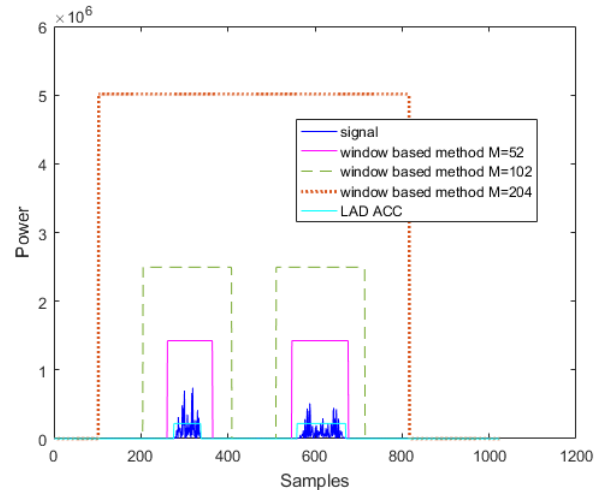


**Figure 8.** One snapshot of two simulated signals with 5% and 10% bandwidth.  $M = 52$  (optimal for 5% BW signal),  $102$  (optimal for 10% BW signal), and  $204$ .

### 4.3. Multipath Channel Scenario

Multipath channel can be a very challenging environment for spectrum sensing since it includes LOS and scattered components (Rician channel) or only scattered components (Rayleigh channel). Let  $a_i, i = 1, \dots, K$  be the average amplitude of each signal component. The total energy of signal components is  $E = \sum_{i=1}^K a_i^2$ . In the case of Rician channel,  $a_1$  is a LOS component and  $a_2, \dots, a_K$  are scattered components. In the Rayleigh channel, there is no LOS (NLOS) component, so all components  $a_i$  are scattered components with some delays.

In the simulations, there were either LOS component and two scattered components (Rician channel,  $K =$

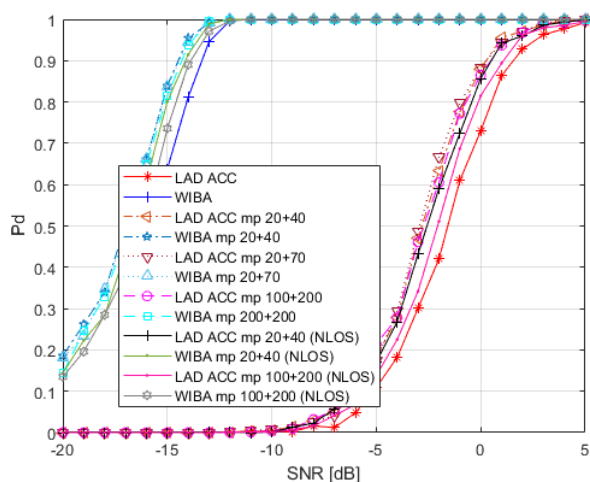


**Figure 9.** Probability of detection vs. SNR in multipath channel case. Signal bandwidth is 10% and  $M = 102$ . AWGN, Rician (LOS) and Rayleigh (NLOS) channels.

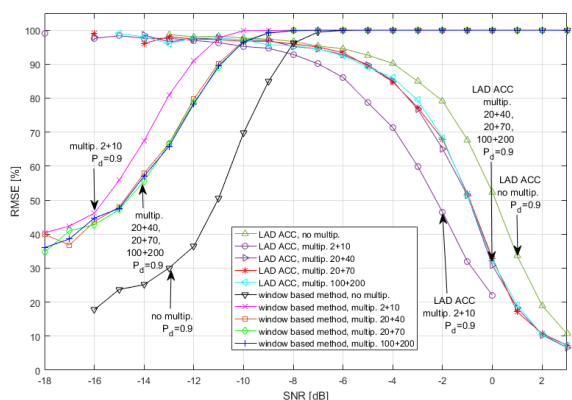


**Figure 10.** RMSE vs. SNR results in the presence of multipath components. BW of the signal is 10% and  $M = 102$ .

3), or only two scattered components (Rayleigh channel,  $K = 2$ ). SNR includes only the energy of first component. In the Rician channel, SNR included the energy of LOS component, first scattered component had energy 3 dB below SNR (i.e. the LOS component), while the second scattered component had energy 6 dB below the SNR (i.e. the LOS component). In the Rayleigh channel, SNR included the energy of first scattered component, and the second scattered component had energy 3 dB below the SNR. Used delays were 2, 20 and 100 samples for the first scattered component, and 10, 40, 70 and 200 for the second scattered component.

In Figure 9, detection probability vs. SNR in Rician and Rayleigh multipath (mp) channel case is considered. Signal BW is 10%,  $M = 102$  (optimal). It can be seen that the multipath enhances the

detection performance by 1 – 2 dB, regardless of the sample delays. This is because constructive summation increases the energy of the signal, and this affects the detection when using ED based methods. In the Rayleigh channel case, there is one component less, so the total energy is less than in the Rician case. Here, SNR is defined to include only the energy of first component. If SNR includes energy of all components, the performance is 1 – 2 dB worse, and the performance equals to the non-multipath performance.

Next, the bandwidth estimation accuracy is studied. In Figure 10, RMSE vs. SNR is presented in the presence of multipath. Here, signal BW is 10% of the channel bandwidth and  $M = 102$  (optimal). This figure also shows the minimum SNR values when the  $P_d \geq 0.9$  is achieved. For example, when there is no multipath and the WIBA method is used, a SNR = –13 dB is required to achieve  $P_d = 0.9$ . As a comparison, the LAD ACC method requires SNR = 1 dB to achieve  $P_d = 0.9$ . The difference between the WIBA and the LAD ACC methods is 14 dB. However, it can be noticed that the LAD method has better BW estimation accuracy. The multipath has about 1 – 3 dB effect to the RMSE performance. The higher SNR is, the better the LAD ACC method finds the signal, and the smaller its RMSE is. Instead, in the case of the WIBA method, the length of the detection window limits RMSE values. As can be seen from the Table 4, RMSE= 100 when detection window length is optimal.

#### 4.4. Rural Area Channel Scenario

The performance of the WIBA energy detector in a challenging rural area channel model for 5G networks was studied in [22]. The results were compared to that of the LAD method. However, there were no results for FSPL AWGN (FSPL) channel case to be used as a comparison point. Here, detection distance in FSPL is studied, and a comparison between rural area and FSPL channels are presented. FSPL is used so that it will be seen what the maximum detection distances are and how much they weaken in the rural channel. That is, FSPL is used to see the upper limit of the detection distance. In the rural area channel model, total bandwidth was 23.4 MHz and carrier frequency was 700 MHz. Path loss model is defined in Section 2.2. Again, signal detection performance target is  $P_d \geq 0.9$ .

In Figure 11, assumed transmit power value of the signal is 30 dBm. When signal BW is 2, 4 or 6 MHz corresponding 8.6%, 17.1% and 25.6% sensing BW, detection distance for the WIBA method is 80, 46 or 32 km in the FSPL channel, respectively. In a rural area channel case, corresponding detection distances are only 2, 1 and 1 km. It means that the detection difference is even 78 km. For the LAD ACC method, corresponding detection distances are 16, 6 and 2 km,

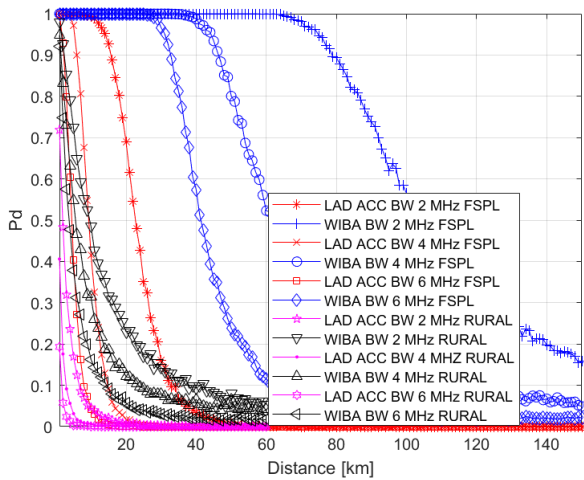


Figure 11.  $P_d$  vs. detection distance when transmit power of the signal is 30 dBm. FSPL and rural channel.

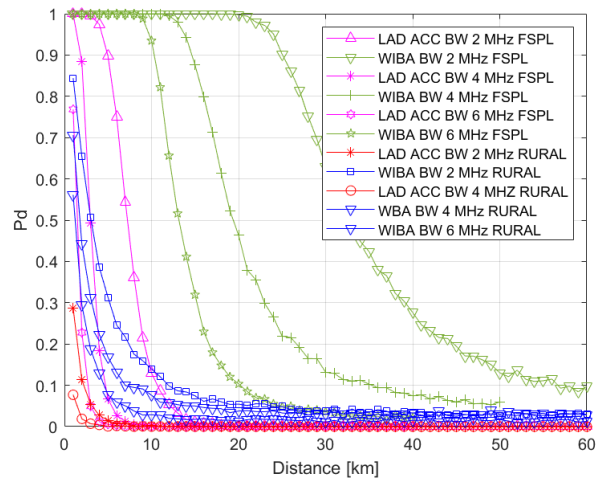


Figure 12.  $P_d$  vs. detection distance when transmit power of the signal is 20 dBm. FSPL and rural channel.

assuming FSPL. In the case of the rural area channel, LAD ACC has  $P_d = 0.45$  at its best.

In Figure 12, assumed transmit power value is 20 dBm. When signal BW is 2, 4 or 6 MHz, detection distance for the WIBA method is 25, 15 or 10 km in the FSPL channel case. In a rural area channel case, signal detection probability is 0.85 at its best, i.e., when signal BW was 2 MHz. For that detection probability, detection distance for the WIBA method is only 1 km. For the LAD ACC method, detection distances are 5, 2 and 0 km in the FSPL channel. In the rural channel, LAD ACC has  $P_d = 0.28$  at its best.

In Figure 13, a transmit power of 10 dBm is assumed. In the FSPL channel case, detection distance is about 3-8 km, depending on BW of the signal. Instead, in a rural area channel case, signal detection probability of the WIBA method is 0.45 as its best.

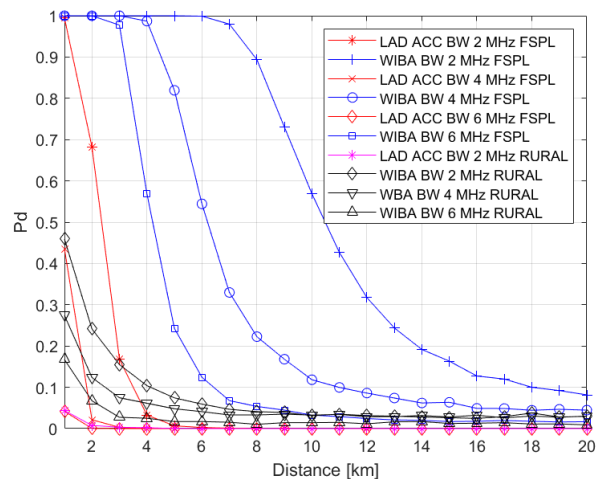


Figure 13.  $P_d$  vs. detection distance when transmit power of the signal is 10 dBm. FSPL and rural channel.

#### 4.5. The Effect of False Alarm Rate

Next, the effect of the false alarm rate to the WIBA method performance is studied when corresponding LAD false alarm rate values for the WIBA method are used. In Figure 14, probability of detection vs. SNR is presented in an AWGN channel. There are three signals with 5% ( $M = 52$ ), 10% ( $M = 102$ ) and 20% ( $M = 204$ ) BWs. The values for the variables  $M$ ,  $L$  and  $P_{fa,desWIBANew}$  can be seen from Table 2. It can be noticed that when the WIBA and LAD ACC methods have equal false alarm rate values, the performance degradation of the WIBA method is around 2 dB.

In Figure 15, probability of detection vs. distance [km] is presented in rural area channel. There is one signal with transmit power 53 or 30 dBm. Bandwidth of the signal is 2 and 6 MHz, and both the WIBA and LAD ACC methods are used. The values for the

variables  $M$ ,  $L$  and  $P_{fa,desWIBANew}$  can be seen from Table 2. When transmit power is 53 dBm, signal BW is 2 or 6 MHz and the WIBA and LAD ACC methods have equal  $P_{FA}$  values, signal can be detected using the WIBA method (final detection probability  $P_{d,i} = 0.9$ ) when Tx-Rx distance is at most 24 or 11 km, respectively. That is, the detection distance is 11 km and 4 km less when compared to results for WIBA  $P_{fa} = 0.01$ , respectively. When transmit power is 30 dBm, signal BW is 6 MHz and the WIBA and LAD ACC methods have equal  $P_{FA}$  values, signal can be detected (final detection probability  $P_{d,i} = 0.85$  because 0.9 is not possible to be achieved) when Tx-Rx distance is at most 1 km. The detection distance is  $< 1$  km when compared to results

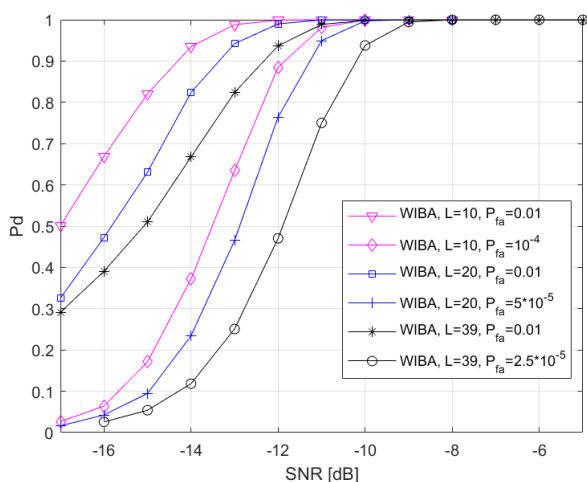


**Figure 14.** Probability of detection vs. SNR [dB] in AWGN channel. The signal bandwidth is 5% ( $L = 39$ ), 10% ( $L = 20$ ) and 20% ( $L = 10$ ).

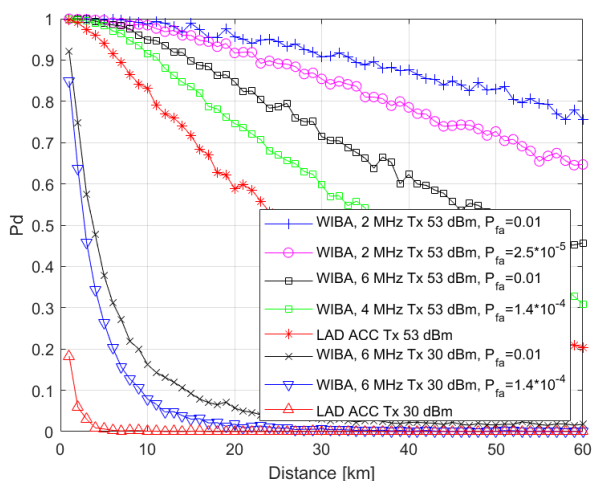


**Figure 15.** Probability of detection vs. distance [km] results. Transmit power of the detected signal is 53 and 30 dBm.

for WIBA  $P_{fa} = 0.01$ . In any case, the WIBA method still outperforms the LAD ACC method.

## 5. Conclusions

Remote and rural area connectivity is a true challenge that can be solved by using lower frequency bands that are made available through shared spectrum access. This would enable cost-efficient solutions for low user density areas. Traditional database-based approach for spectrum sharing can be enhanced by introducing spectrum sensing to more accurately characterize the current spectrum usage in order to identify more opportunities for shared spectrum access. It can enhance the detection of existing spectrum users

as well as the detection of other newly introduced spectrum users. In this work, the performance of a spectrum windowing based energy detection method WIBA was studied, and comparison was made with the well-studied LAD ACC method. Probability of detection, relative mean square error for the bandwidth estimation, and the number of detected signals as well as detection distances were evaluated. In addition, false alarm rate analysis was also presented. It can be concluded that the WIBA method has better detection probability than the LAD ACC method. The WIBA method is able to operate with SNR below  $-10$  dB, depending on the signal and window lengths. The WIBA method is suitable for 5G applications especially for rural and remote areas due to its good detection performance in low SNR areas. It can enhance the accuracy of spectrum usage information to complement the database approach. The effect of the detection window length to the detection performance in different channel situations was also studied. Too long detection window degrades the performance of the WIBA method. The LAD ACC method outperforms the WIBA method in terms of bandwidth estimation accuracy. Therefore it can be concluded that if signal detection at a given frequency band is enough for the system, the WIBA method is preferred. If bandwidth estimation accuracy is important, the LAD ACC could be used after the WIBA method to improve the bandwidth estimation.

**Acknowledgement.** This research has received funding from the European Union Horizon 2020 Programme (H2020/2017-2019) under grant agreement N0. 777137 and from the Ministry of Science, Technology and Innovation of Brazil through Rede Nacional de Ensino e Pesquisa (RNP) under the 4th EU-BR Coordinated Call Information and Communication Technologies through 5G-RANGE project. In addition, this research has been financially supported in part by Academy of Finland 6Genesis Flagship (grant 318927) and CNPq-Brasil.

## References

- [1] VARTIAINEN J., KARVONEN H., MATINMIKKO-BLUE M. and MENDES L. (2019) Performance Evaluation of Windowing Based Energy Detector in Multipath and Multi-Signal Scenarios. *In Proceedings of Crowncom 2019*, Poland, pp. 59–72.
- [2] BOCKELMANN C. *et al.* (2018) Towards Massive Connectivity Support for Scalable mMTC Communications in 5G Networks. *IEEE Access*, vol. 6.
- [3] 5G-RANGE project, <http://5g-range.eu/>. Last accessed 30 Mar 2020
- [4] KLIKS A. *et al.* (2019) Database Supported Flexible Spectrum Access - Field Trials in Commercial Networks. *In Proceedings of IEEE ICC Workshops 2019*, pp. 1–6.
- [5] HU F., CHEN B., and ZHU K. (2018) Full Spectrum Sharing in Cognitive Radio Networks Toward 5G: A Survey *IEEE Access* vol. 6, pp. 15754–15776.

- [6] XIN C., PAUL P., SONG M. and GU Q. (2019) On Dynamic Spectrum Allocation in Geo-Location Spectrum Sharing Systems. *IEEE Transactions on Mobile Computing* vol. 18, pp. 923–933.
- [7] YAMASHITA S., YAMAMOTO K., NISHIO T., and MORIKURA M. (2018) Exclusive Region Design for Spatial Grid-Based Spectrum Database: A Stochastic Geometry Approach. *IEEE Access* vol. 6, pp. 24443–24451.
- [8] ZAERI-AMIRANI M., AFGHAH F., and ZEDADALLY S. (2018) A Hierarchical Spectrum Access Scheme for TV White Space Coexistence in Heterogeneous Networks. *IEEE Access* vol. 6, pp. 78992–79004.
- [9] ZHANG W., ZHANG G., ZHENG Y., YANG L., and YEO C.K. (2018) Spectrum Sharing for Heterogeneous Networks and Application Systems in TV White Spaces. *IEEE Access* vol. 6, pp. 19833–19843.
- [10] FCC (2015) Amendment of the Commission’s Rules with Regard to Commercial Operations in the 3550–3650 MHz Band. *In Report and Order, FNPRM*, FCC-15-47.
- [11] CERRO G., and MIELE G. (2019) A stand-alone sensor for spectrum occupancy monitoring in dynamic spectrum access framework. *In Proceedings of IEEE SAS 2019*, pp. 1–6.
- [12] HOLLAND O. et al. (2018) 5G Needs Database-Driven Spectrum Sharing!. *In Proceedings of IEEE International Symposium DySPAN 2018*, pp. 1–10.
- [13] LI B., LI S., NALLANATHAN A. and ZHAO C. (2015) Deep Sensing for Future Spectrum and Location Awareness 5G Communications. *IEEE Journal on Selected Areas in Communications* vol. 33, num. 7, pp. 1331–1344.
- [14] ATAT R., LIU L., CHEN H., WU J., LI H. and YI Y. (2017) Enabling cyber-physical communication in 5G cellular networks: challenges, spatial spectrum sensing, and cyber-security. *IET Cyber-Physical Systems: Theory and Applications*, vol. 2, Iss. 1, pp. 49–54.
- [15] EJAZ W. and IBNKAHLA M. (2018) Multiband Spectrum Sensing and Resource Allocation for IoT in Cognitive 5G Networks. *IEEE Internet of Things Journal*, vol. 5, no. 1, pp. 150–163.
- [16] VARTIAINEN J., HOYHTYA M., VUOHTONIEMI R. and RAMANI V.V. (2016) The Future of Spectrum Sensing. *In Proceedings of ICUFN 2016*, pp. 247–252.
- [17] AKYILDIZ I.F., LO B.F., and BALAKRISHNAN R. (2011) Cooperative Spectrum Sensing in Cognitive Radio Networks: A survey. *Physical Communication*, vol. 4, no. 1, pp. 40–62.
- [18] LIU X., HE D. and JIA M. (2017) 5G-based wideband cognitive radio system design with cooperative spectrum sensing. *Physical Communications*, vol. 25, part 2, pp. 539–545.
- [19] SAARNISAARI H. and VARTIAINEN J. (2018) Spectrum Window Based Signal Detection at Low SNR. *In Proceedings of ICMCIS 2018*, Poland.
- [20] VARTIAINEN J., LEHTOMAKI J.J. and SAARNISAARI H. (2005) Double-threshold based narrowband signal extraction. *In Proceedings of VTC fall 2001*, pp. 1288–1292.
- [21] VARTIAINEN J. (2010) Concentrated signal extraction using consecutive mean excision algorithms. In: Ph.D. Dissertation, Acta Univ Oul Technica C 368. Faculty of Technology, University of Oulu, Finland.
- [22] VARTIAINEN J., MATINMIKKO-BLUE M., KARVONEN H. and MENDES L. (2019) Performance of WIBA Energy Detector in Rural and Remote Area Channel. *In Proceedings of ISWCS 2019*, pp. 1–5.
- [23] VARTIAINEN J., KARVONEN H., MATINMIKKO-BLUE M., MATOS A. and SILVA C. (2019) Cooperative Sensing With WIBA Energy Detection Under Rural Area Channel Conditions. *In Proceedings of VTC fall 2019*, pp. 1–6.
- [24] ECC (2011) Technical and operational requirements for the possible operation of cognitive radio systems in the white spaces of the frequency band 470-790 MHz. *In ECC Report 159*.
- [25] Ericsson and Telstra (2016) Measurements of Extreme Rural Scenarios. R1-166599.
- [26] PESSOA A.M. et al. (2019) CDL-based Channel Model for 5G MIMO Systems in Remote Rural Areas. *In 16th International Symposium on Wireless Communication Systems (ISWCS)*, Finland, pp. 21–26.
- [27] SOKAL B et al. (2018) D3.1 Physical layer of the 5G-RANGE – Part I, 5G-RANGE Project deliverable.
- [28] Ericsson and Telstra (2016) Channel model for extreme rural scenario, R1-167451.
- [29] 3rd Generation Partnership Project (3GPP) (2018) Study on channel model for frequencies from 0.5 to 100 GHz, TR38.901, v15.0.0.
- [30] MILLER K.S. (1969) Complex Gaussian Process. *Siam Review* vol 11, pp. 544–567.
- [31] NEESER F.D. and MASSEY J-L. (1993) Proper complex random processes with applications to information theory’. *IEEE Transactions on Information Theory*, vol. 39, pp. 1293–1302.
- [32] LEHTOMAKI J.J., VARTIAINEN J., JUNTTI M. and SAARNISAARI H. (2003) CFAR outlier detection with forward methods. *IEEE Transactions on Signal Processing* vol. 55, pp. 4702–4706.
- [33] SAARNISAARI H. and HENTTU P. (2003) Impulse detection and rejection methods for radio systems. *In Proceedings of MILCOM 2003*, pp. 1126–1131.
- [34] PROAKIS J.G. (1995) Digital Communications. 3rd ed. (McGraw-Hill, Inc.).